Reverberation and Absorption in an Aircraft Cabin with the Impact of Passengers

Andersen, Jørgen Bach; Chee, Kin Lien; Jacob, Martin; Pedersen, Gert Frølund; Kurner, Thomas

Published in:
I E E E Transactions on Antennas and Propagation

DOI (link to publication from Publisher):
10.1109/TAP.2012.2189700

Publication date:
2012

Document Version
Early version, also known as pre-print

Reverberation and Absorption in an Aircraft Cabin with the Impact of Passengers

Jørgen Bach Andersen, *Life Fellow, IEEE*, Kin Lien Chee, *Member, IEEE*, Martin Jacob, *Student Member, IEEE*, Gert Frølund Pedersen, *Member, IEEE*, Thomas Kürner, *Senior Member, IEEE*

***Abstract*—Using a similar approach to that applied in acoustics and in microwave reverberation chambers, a theory of wideband propagation in a closed environment is discussed. Here, a room environment is viewed as a lossy cavity, characterized by diffuse scattering from walls and internal obstacles. For experimental results, measurements from 3 to 8 GHz were performed in a 24 passenger section of an aircraft cabin. This UWB system has the transmitter at ceiling height and the receivers at armrest and headrest positions. The measurements were performed for the cabin being unoccupied and fully occupied. In the theoretical model, the closed room environment is characterized by the reverberation time and volume, and these parameters allow derivation of the the remaining parameters such as path loss and average passenger absorption. The RMS delay spread and mean excess delay are also studied. For the mean power the agreement between the theory and measurements is good to within 1-2 dB, indicating the excellent accuracy of the method, which extends to estimating body absorption in real world environments. The total absorption from the seated passengers is dominated by the few who are near the transmitter. In general, this absorbed power is relatively small, so the effect of passengers is marginal for this configuration of a cabin communication system.**

***Index Terms*— UWB propagation, room acoustics, room electromagnetics, diffuse scattering.**

I. Introduction

INDOOR microwave propagation has been treated in detail for many years [1]. Different approaches exist covering statistical models based on measurements as well as deterministic models like ray tracing. In order to analyze the propagation channel of a wideband communication system the impulse response is the most important characteristic used, since system parameters like the RMS delay spread can be derived from the data. Modeling of the impulse response has previously involved a time domain cluster model [2] and the cluster model has been extended to include clustering in the angular domains in the WINNER project [3]. Simple statistical models for wideband path loss modeling and delay parameter determination have been developed for standardization [4-6]. In these models a finite number of rays (plane waves) exist. In the approach presented in this paper only the LOS part exists together with a single cluster in delay and uniform angular distribution. A numerical model has recently been published, which supports these assumptions [7]. A multidimensional measurement approach [8] describes a number of discrete paths together with an exponential decay component, ascribed to diffuse scattering, and which is termed dense multipath. This result is also close to the presented work, except that here only one coherent component exists, the LOS from the transmitter, if not shadowed.

Ray tracing is a popular method [9] but it has difficulties with rough surfaces. In terms of scattering it is important to distinguish between coherent scattering from the walls and diffuse scattering from random objects and rough surfaces. Most ray tracing methods rely implicitly on coherent reflections from smooth surfaces allowing image methods to be applied. Our goal is to represent this diffuse scattering in the simplest way but still encompassing all essential features of closed-room propagation. Thus, our model considers a first-arriving LOS signal, if present, while multiple reflections and scattering gives rise to a tail with exponential decay and a time constant noted as the reverberation time, similar to the acoustic case; see Fig. 1, where t_0 (time of flight) denotes the arrival time at a specific position.

Full wave solutions can be obtained numerically for simplified environments [10], however, it requires high detail of the full configuration of the environment which in many cases is not feasible. The method applied in this paper seeks a very simple model, with only few parameters needed for a description of the propagation. The indoor environment is considered as a lossy cavity where all the effective losses can be described with a single parameter. The method has been previously applied to a single large office environment [11, 12] and was coined "Room Electromagnetics" analogous to the well-known "Room Acoustics" [13]. The acoustics community has been applying the method since the 1920's (Sabine's equation), so it is surprising that it has not been used earlier by the microwave community, considering that the fundamental difference from acoustic wave modeling is only the polarization. In the Appendix, the differences and similarities between acoustics

Manuscript received December 15, 2010. The research leading to these results has received funding from the European Union's Seventh Framework Programme ([FP7/2007-2013]) under grant agreement n° 244149.

Published in IEEE Transactions on Antennas and Propagation, Vol. 60, No. 2, p. 633–643, February 2012. DOI: 10.1109/TAP.2011.2173435.

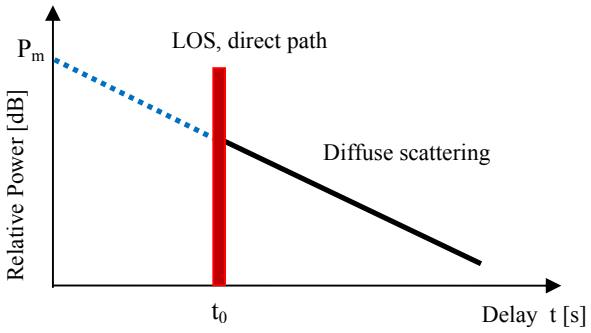

Fig. 1: Modeling of mean impulse response consisting of a direct LOS path and an exponential tail of diffuse scattering with time constant τ.

and electromagnetic are further elaborated.

Considerable research has been undertaken on microwave reverberation chambers, e.g., [14], which are enclosures with stirring to randomize the field distribution. Reverberation chambers are not necessarily governed by diffuse scattering, which is the main contribution in this paper. The measurement data used in this paper have been published before in [15, 16] with a standard type of modeling, but are applied here to give additional insights using a different theory.

It is noteworthy that in theory [12], the tails of the impulse response ($t>t_0$) for a specific room, have the same exponential slope and power level, regardless of position within the room. It is also independent of the antenna radiation pattern. This idea originates from experimental observations [12] and is well supported by the acoustics theory.

In this paper, measurements in an aircraft cabin are compared with the proposed theory and the effects of passengers in the seats are also investigated. The propagation of a UWB channel within a passenger cabin was previously studied in [17, 18], whereas the effect of human presence in a midsize airliner was previously investigated in [19]. One of the drawbacks common to these previous investigations is the lack of a simple theory which allows effective quantification of the influence of the human occupants on UWB propagation.

The paper is organized as follows. Section II presents a brief theory of room electromagnetics with more details in the Appendix. A description of the cabin and measurement scenario is presented in section III. A comparison between calculation from theory and measurements is presented in section IV. Section V summarizes the observations and concludes the paper.

II. Theory of Diffuse Radiation

The theory relies heavily on the developments from acoustics [13]. The relationship to acoustics and derivation of the mathematical results are given in the Appendix. Here we shall just give an overview, clarifying the assumptions.

A rough wall may reflect electromagnetic waves in two ways, (i) a coherent component, which for planar structures may be computed by the Fresnel reflection coefficients and the use of image theory, and (ii) an incoherent scatter from all scatterers in all directions. The value of the reflection coefficient will decrease as the roughness increases. It is assumed here that the roughness (or randomness) is so large that the diffuse part dominates. In the time domain, multiple scattering leads to an exponential decay of power with a decay constant, τ, called the reverberation time. This can be obtained from (A9)

$$\tau = \frac{4V}{cA'} \tag{1}$$

where V is the room volume, A' the effective absorption area, and c the velocity of light. A' may also be written as ηA, where A is the true surface area and η is the absorption coefficient. The power at zero delay, P_m in Figure 1, is given in (A14) by

$$P_m = \frac{\lambda^2}{(4\pi)^2}\frac{c\Delta}{V}\eta_{pol} \tag{2}$$

where impulse width, Δ, is much smaller than the reverberation time. η_{pol} is a factor giving the fraction of the incident power at the antenna that matches the polarization of the antenna. The field is assumed to be completely random, including the polarization, so $\eta_{pol}= 0.5$. The distributed (over the full sphere) directivity of the antennas equals one, since the incident energy is assumed uniformly distributed over all directions. The antennas are assumed lossless.

In order to find the received power, P_{rec}, we need to integrate the impulse over the delay time (A13)

$$\frac{P_{rec}}{P_{in}} = \frac{\lambda^2}{4\pi^2 A'}e^{-t_0/\tau}\eta_{pol} = \frac{\lambda^2}{8\pi^2 A'}e^{-t_0/\tau} \tag{3}$$

III. Measurement Scenario

A measurement campaign was carried out at the front section, upper deck of a double-decker large wide-bodied aircraft mockup. The investigated area of the cabin consists of five rows of seats and, depending on the row number, each has up to six seats which leads to a total of twenty-four seats. A staircase to gain access to the lower deck is located at the front of the investigated area while the end of the investigated area was covered up by wooden doors. Fig. 2(a) and 2(b) show the layout of the aircraft cabin with transmitter positions marked with a solid rhombus and receiver positions indicated by solid rectangles. Owing to the longitudinal symmetry of the aircraft cabin, transmitters were located at only one of the side walls, at the front (E1 from Fig. 2(a)) and at the end (E3 from Fig. 2(b)).

All transmitters were raised to ceiling height on a tripod while receivers were mounted at headrest and armrest heights, aiming to differentiate LOS and NLOS propagation scenarios. Channel measurements were first performed in an empty cabin and then the measurement was repeated in a fully occupied

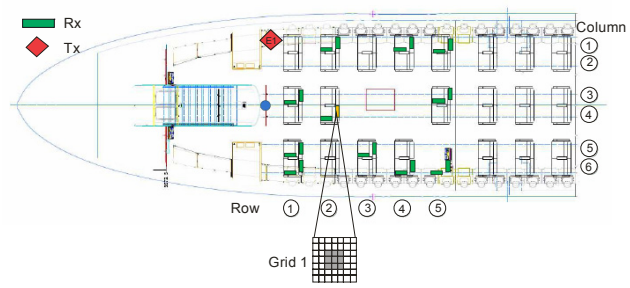

Fig. 2(a): Cabin layout with transmitter E1 located at the front. Receivers (Rx) were located at headrest and armrest height. Additional grid measurements were performed at Grid 1 at headrest height.

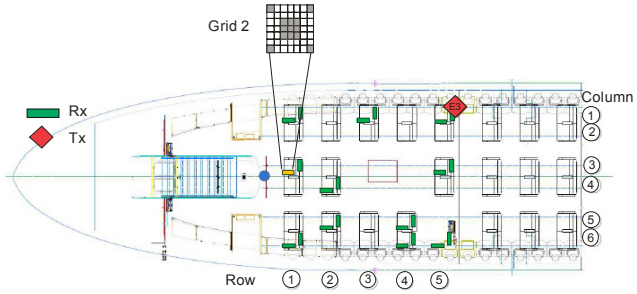

Fig. 2(b): Cabin layout with transmitter E3 at the end of the cabin section which was shielded. Receivers (Rx) are located at headrest and armrest height. Additional grid measurements were performed at Grid 2 at armrest height.

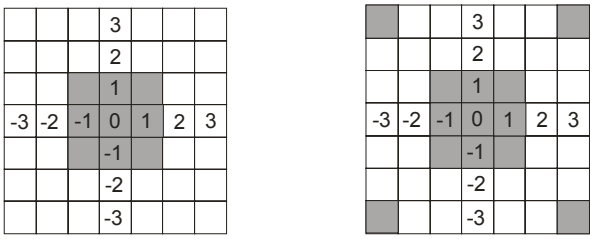

Fig. 3(a) and 3(b): 9 measured positions from Grid 1(left) and 13 measured positions from Grid 2 (right).

cabin (all 24 seats with a passenger).

With the aim of ensuring that the small-scale fading characteristics were captured within a local area, two gridded measurements were conducted at two different seats in the aircraft cabin. The measurements were performed with the aid of measurement tools known as Grid 1 and Grid 2. These comprise 7 x 7 grids with each cell spaced by 40 mm as shown in Fig. 3(a) and 3(b). During these measurements, Grid 1 was at the headrest (HR) position while Grid 2 was mounted at armrest (AR) position. With the grid spacing being close to half of the wavelength of the lowest frequency, the aim is to ensure the spatial samples collected are uncorrelated. It has been reported in [15, 16] that the small-scale fading can be effectively averaged out from 9 spatial grid samples, so that the shape of the mean power delay profile can be estimated. Therefore, 9 positions from Grid 1 and 13 positions from Grid 2 were measured. The transfer functions of the channel were measured using a vector network analyzer (Rohde & Schwarz

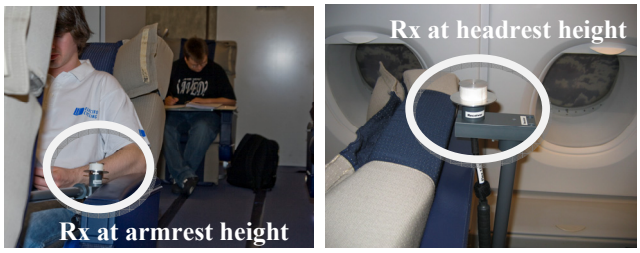

Fig. 4(a)(b): Receiver at armrest height in fully occupied cabin (left) and receiver at headrest height in empty cabin (right).

ZVC, 20 kHz-8GHz) for a frequency range from 3 to 8 GHz. In order to increase the dynamic range of the setup, the output signal of the VNA was amplified by about 50 dB using an HF amplifier (PTC6345-N from TMD). The measurement setup is depicted in Figure 5. In order to exclude the influence of the amplifier and all cables used for the measurement, the calibration planes are at the ends of the cables as shown in Figure 5. Small conical antennas with good impedance matching over the frequency band were used during the measurement and the almost frequency-independent antenna patterns are included in the channel. The patterns are omnidirectional in the horizontal plane, and they capture, for the experimental channel transfer functions, the vertically polarized components from these directions. The horizontal polarization and the incident components from the other directions are suppressed according to the pattern.

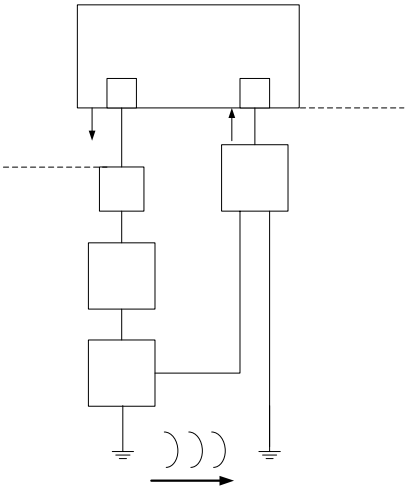

Fig. 5: Measurement setup used in the measurement campaign.

IV. COMPARISON WITH MEASUREMENTS

A. Reverberation Time

The reverberation time may be derived from the measurement data using the slope in dB/ns. Fig. 6 shows sample (instantaneous) impulse responses measured from one access point (E3) to three different occupied seats. The resolution is 0.2 ns corresponding to the total bandwidth of 5 GHz. The straight line is the best minimum least-square fit to all three curves between 40 and 140 ns to avoid the LOS and the noise

floor, respectively The slope of the best fit line corresponds to a reverberation time of $\tau = 17.7$ ns.

The receiver located at the nearest seat {(row, column) = (5, 1)} has a LOS link to the transmitter, hence the impulse response is dominated by the LOS component and close proximity scatterers contributing to the beginning of the impulse response. This deviates very much from the impulse responses measured from the other receivers at seat (2, 4) and seat (1, 1). After about 25 ns, however; all the three tails are about the same, both in slope as well as in amplitude, which supports the general diffuse theory. Owing to the lack of spatial averaging in these sample results, there is considerable variability. However, this can be resolved by using the data obtained from grid measurements for two seats as mentioned above; the frequency dependence is studied with a bandwidth of 1 GHz. Following the model, the exponential decay of the diffuse component is approximately the same regardless of the measured positions as indicated earlier, and only the grid measurement data set derived from one of the seats (2, 4) with transmitter E1 is shown. The dependence of reverberation time on frequency, as well as on seat occupancy, is depicted in Fig. 7, where the reverberation time, derived by best-fitting the measured averaged impulse responses is found to fall between 15 ns and 25 ns. The decline of reverberation time with frequency is an indication of increasing absorption with frequency (A9).

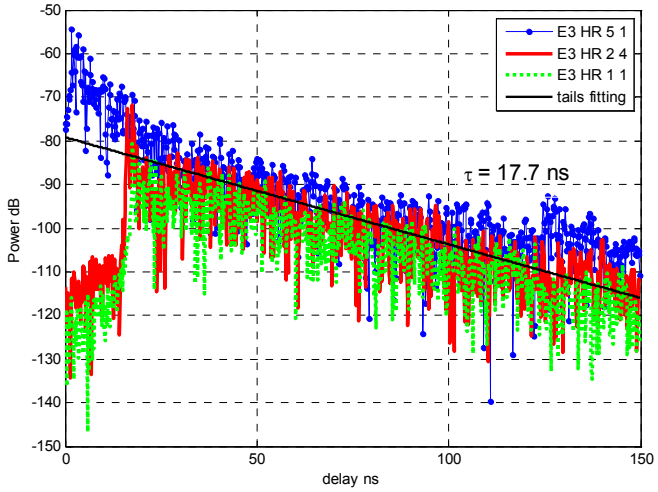

Fig. 6: Impulse responses measured from one access point to different seats in headrest (HR) positions, where seat = {(row, column)| (5,1), (2,4) and (1,1)}. The responses are derived from 1600 frequency points from 3 to 8 GHz. The arrival times correspond approximately to the distances between the antennas. The average slope of the tails corresponds to an average reverberation time of 17.7 ns.

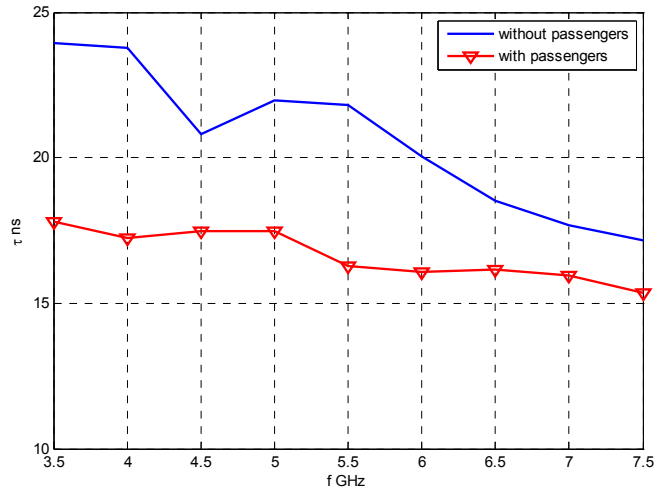

Fig. 7: Reverberation times as a function of frequency and occupancy of seats averaged over 13 closely spaced points in a grid [12]. Bandwidth used is 1 GHz.

From a communication point of view, the reverberation time τ is not the only time parameter of interest - others are the RMS delay spread s and the mean arrival time t_m

$$t_m = \frac{\int tP(t)dt}{\int P(t)dt} \qquad s = \sqrt{\frac{\int (t-t_m)^2 P(t)dt}{\int P(t)dt}} \tag{4}$$

where t is the arrival time of a point on the delay axis and $P(t)$ is the corresponding power. The excess delay is the mean arrival time minus the propagation delay (time of flight), t_m-t_0.

For the simple model of Figure 1 it is easy to find the various moments analytically with the result that

$$s = \frac{\tau}{\sqrt{K+1}} \tag{5}$$

$$t_m - t_0 = \frac{\tau}{K+1}. \tag{6}$$

so the delay spread is upper bounded by the reverberation time and lower bounded by the mean excess time, in good agreement with figure 8 for the fully occupied cabin. K is the Ricean K-factor.

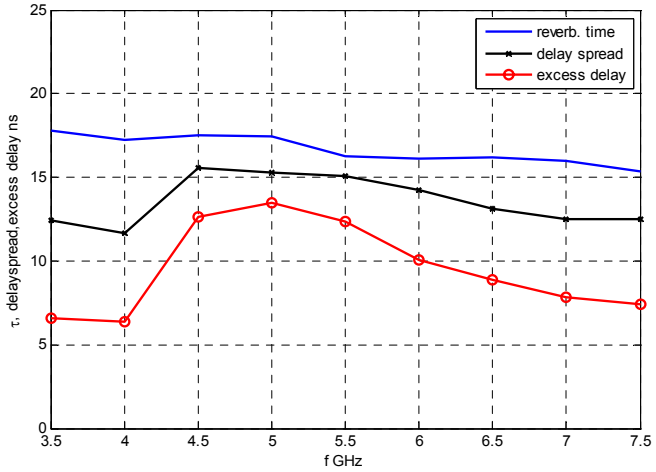

Fig. 8: Three characteristic time parameters for a fully occupied cabin. The delay spread and the excess arrival time are smaller than the reverberation time owing to the concentration of the impulses near the beginning. For a strictly exponential curve, K=0, the three parameters would be identical.

B. Path Loss

In order to determine the average path loss corresponding to the diffuse power from eq. (A13), we need to determine the volume V, the reverberation time τ, and the distance d_0. τ is determined from the measured impulse responses and distance d_0 is the shortest distance between receiver and transmitter. In an ordinary room, the volume can be easy to measure, but for a complicated structure such as an aircraft cabin with cylindrical cross section, furniture clutter, and openings to other levels, it is not simple. It is interesting to observe from eq. (A14) that for an impulse which is shorter than the reverberation time ($\Delta << \tau$), the level of the exponential tail of the impulse response depends on the volume and wavelength only. With a pulse width Δ of 0.2 ns used in our discussion here, this condition is satisfied, and the volume V is estimated to be 100 m^3 from eq. (A14).

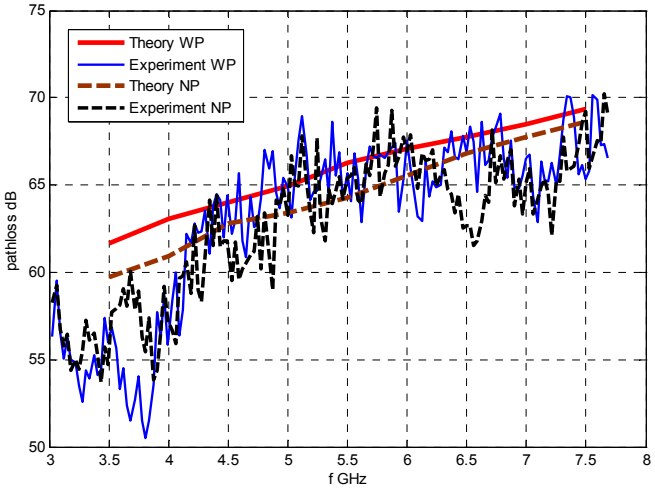

Fig. 9a: Diffuse path loss at headrest E1 as function of carrier frequency for a fully occupied (WP) and an unoccupied (NP) cabin.

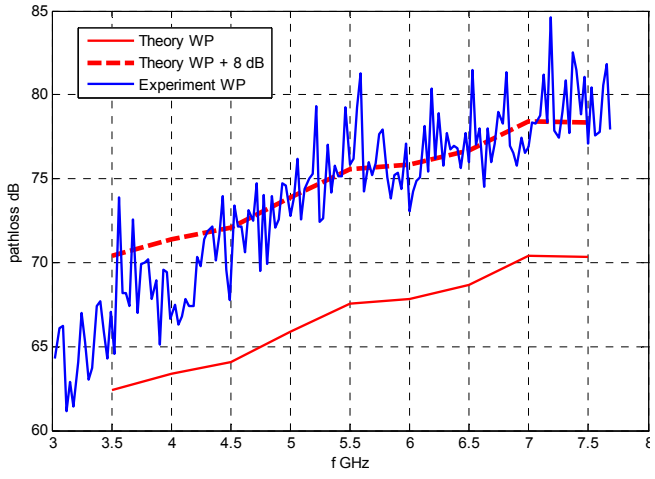

Fig. 9b: Diffuse path loss at armrest E3 for a fully occupied cabin (WP). An additional armrest shadowing loss of 8 dB compared with headrest position.

In Fig. 9a, the theoretical path loss for diffuse power is compared with an experiment for a full (WP=With Passengers) and unoccupied cabin (NP=No Passengers), using the reverberation times from Fig. 7. The first observation is that, from a path loss point of view, the difference between fully occupied and unoccupied is in the order of 1 to 2 dB. One dB can be accounted for by the reduction of τ by about 20% (Fig. 7), and the remaining loss comes from the exponential spatial decay (last factor in (A12)). The frequency dependence is dominated by the λ^2 term in the path loss (A13), although τ is also somewhat frequency dependent. The path loss exhibits an additionally drop at frequencies below 3.5 GHz for an unknown reason.

In Fig. 9b, the armrest scenario in an occupied cabin is shown. The measurement result shows an additional loss of about 8 dB for this particular location, which may be interpreted from the fact that the field of view is limited at armrest level so not all the multipath rays may reach the antenna, in contrast to the headrest with a wider field of view. This additional loss has also been noted in [15].

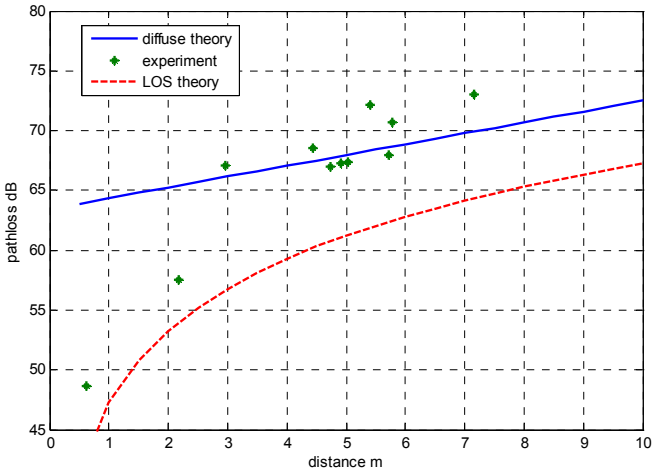

Fig. 10: Path loss versus distance with occupied cabin, antenna at headrest, f=5.5 GHz. The LOS case assumes a directivity of 1 and dominates at small distances. Averaging over a 200 MHz bandwidth. τ is set at 16 ns.

The spatial variation of the path loss is also important and an example is shown in Fig. 10 with antennas at headrest level for a full cabin scenario. In order to reduce the variability, the powers are averaged over a 200 MHz bandwidth centered at 5.5 GHz. Both the power law of LOS and the exponential law for the diffuse radiation (A13) are shown. It is clear that the LOS strongly dominates at short distances of 1-2 meters, while the diffuse radiation dominates at larger distances. The agreement is reasonable, but it is of course apparent that other models may also be used to explain the situation, such as those discussed in [14, 15]. However, the presented model has the advantage of a physical mechanism as its basis. The slope of the diffuse power versus distance can be derived from (A13) with $t_0=d_0/c$

$$\frac{dP(dB)}{dl} = \frac{10}{\log(10)\,\tau\,c} \quad [dB/m] \qquad (7)$$

which equals 0.9 dB/m for τ =16 ns, for the case of Fig.10.

C. *Absorption in Persons*

There are two aspects of the presence of seated passengers: the propagation parameters such as path loss and delay spread are influenced; and some of the energy is absorbed. The latter aspect is discussed in this section, since possible health risks continue to be an issue. The relevant concern here is the whole- body Specific Absorption Ratio (SAR) which depends on absorbed power per unit weight. The SAR is often found numerically [22] from knowledge of the distribution of complex permittivity in the body, and experimental values are scarce. The absorbed power is the product of the incident intensity I (W/m^2) and the absorption cross section A_p (m^2) of a person. The measurements described in this paper allow us to quantify the absorption in a single passenger by assuming that the absorption cross section of each passenger is the same.

Having already determined the reverberation times (Fig. 7) the absorption areas for a full and empty cabin may be found from eq. (A9), and the result is shown in Figure 11. There is a clear difference between the fully occupied and unoccupied cabin, and we assume that the difference is purely due to the absorption of the passengers. The total amount of absorbed power relative to transmitted power is around 0.10-0.27, since the total transmitted power must equal the total absorbed power.

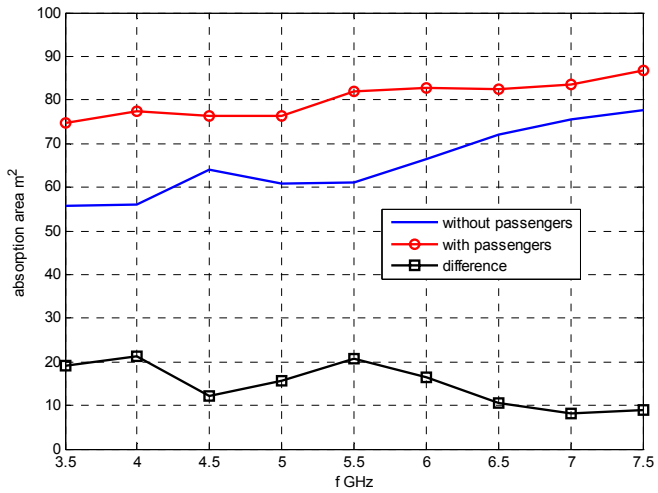

Fig. 11: Absorption areas for a full and an empty cabin based on reverberation times (Fig. 7). Headrest at grid E1. The difference curve is assumed to be due to absorption in passengers. In this case 10-27 % of the input power is absorbed by passengers.

The relevant quantity we need is the intensity I_i incident on the passenger, and this may be derived from the received power by dividing with the antenna absorption area. It should be noted that the polarization factor should not be applied since both polarizations contribute to the absorbed power. The intensity relative to 1 Watt transmitted power is shown in Figure 12 as a function of distance from the access point, the figure is essentially the inverse of Fig. 10, the equation relating the relative absorbed power with the intensity and the absorption area of the persons is then (A6)

$$\sum_{i=1}^{24} I_i \pi A_p = \pi A_p \sum_{i=1}^{24} I_i = 0.25 \qquad (8)$$

where the index i refer to passengers, and 0.25 a representative number for the relative absorbed power. The problem is that we do not know the intensity (or received power) at all the seats, but a good estimate is sufficient for a simple model. Assume that two persons are exposed with I_i=*0.1* W/m^2, two with I_i=*0.01* W/m^2, and 20 persons with I_i=*0.001* W/m^2, which is in rough agreement with Fig. 12. The resulting A_p from eq. 8 is then *0.33* m^2. This area is in good agreement with experimental results such as [17] where a figure of *0.4* m^2 is quoted at 2.4 GHz with the note that the result "varies very slowly with frequency". In [18] an absorption cross section of *0.38* m^2 is computed for adult Japanese for a frequency of 2 GHz.

After having determined A_p, we may also note that the total absorption will fall drastically if no passenger is located within 2 meters from the access point. In this example, the total relative power absorbed by the persons will drop to 0.06 instead of 0.25, when the two closest persons are moved from a position with incident intensity at 0.1 W/m^2 to another position with incident intensity at 0.01 W/m^2.

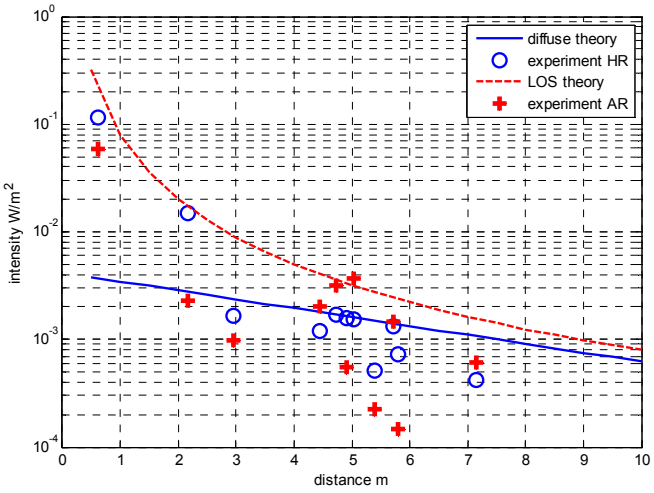

Fig. 12: Intensity in W/m^2 for 1 W input as a function of distance. Essentially the same as the negative of Fig. 10 corrected for antenna area and polarization.

V. CONCLUSION

A simple method for addressing the impact of persons is presented in this paper. The theory is inspired by the observation that in closed rooms the acoustic impulse response features a single exponential tail where the level and slope of the tail is essentially the same everywhere in the room. This leads to the equivalent electromagnetic theory for rooms. The approximations made are:

- The effect of polarization is included by assuming that it is completely random. This makes the theory very similar to room acoustics.

- Incoherent diffuse scattering is assumed to be valid everywhere within the room. This makes the theory different from standard ray tracing techniques and the use of image theory for coherent reflections.

These approximations make the theory very simple and similar, but not identical, to microwave reverberation chamber theory. The theory considers the use of finite pulse width for exciting the impulse response which leads to a spatial distribution of the diffuse energy (in a narrowband steady state situation the diffuse power is uniformly distributed). From the assumption of diffuse scattering, an experimentally determined reverberation time allows determination of the path loss and delay time parameters. The theory is compared with accurate experimental results measured over a 5 GHz bandwidth in an unoccupied and fully occupied cabin, and the agreement is within a few dB for path loss. When the antenna is 'buried' in the environment so not all paths are visible an additional loss is noted. In close proximity to the transmitter, the field intensity is dominated by the LOS component. The diffuse power becomes dominant further away from the transmitter, so in general the total absorption depends critically on any people that are in close proximity to the transmitter. The average absorption area of a passenger has been approximately determined for a fully occupied aircraft cabin section, but the method is general and applies to other indoor single room spaces.

APPENDIX

The following is a condensed version of the theory of diffuse radiation as developed by [13], with the proper modifications required to go from acoustics to electromagnetics. The theory of electromagnetic reverberation chambers [14] is closely related.

The main difference and similarity between acoustics and electromagnetics can be shown through the basic differential equations for free space [23]

$$\nabla^2 \overline{A} + k_e^{\,2} \overline{A} = 0 \tag{A1}$$

$$\nabla^2 p + k_a^{\,2} p = 0 \tag{A2}$$

where $\overline{A}$ is the electromagnetic vector potential (not to be confused with absorption area, A) and p the acoustic pressure. In the case of only vertical polarization, say, $\overline{A}$ will be a scalar. The wavenumbers are $k_e=\omega/c$ and $k_a=\omega/v$, ω being the angular frequency, c the velocity of light, and v the velocity of sound, so the wavenumbers or wavelengths ($\lambda=2\pi/k$) are of the same order. Of course their material properties may be different, but the approximate equality of the wavelengths indicates that the correlation properties of the surfaces are similar. The phase of the waves is not relevant because diffuse scattering relates to the local mean power.

The basic assumption is complete randomness for the diffuse tail of the impulse response, which can be translated into uniformly distributed directions of intensity I (W/m^2) at any time. The energy density is [23]

$$W = W_e + W_m = \frac{1}{4}\varepsilon|E|^2 + \frac{1}{4}\mu|H|^2 = \frac{I}{c} \tag{A3}$$

for one incident path, so for many paths we integrate over all directions

$$W = \frac{1}{c}\iint I(\vartheta,\varphi)\sin\vartheta d\vartheta d\varphi = 4\pi\frac{I}{c} \text{ [W s/m}^3\text{]} \tag{A4}$$

since we assume that all directions carry the same intensity I.

Assume now that the intensity in (A3) is incident on a wall area A, which partly absorbs it with fraction η. The total power absorbed is an integration over a half-space (one side of the wall), i.e.

$$P_{abs} = \eta\, A\int_0^{2\pi}\int_0^{\pi/2} I(\vartheta,\varphi)\cos(\vartheta)\sin(\vartheta)d\vartheta d\varphi \text{ [W]} \tag{A5}$$

where the cosine term is needed for defining the apparent aperture in the direction ϑ. Since I is independent of direction,

$$P_{abs} = A'\pi\, I = \frac{cA'}{4}W \text{ [W]} \tag{A6}$$

where we have introduced $A' = \eta A$.

With an input source power of $P_{in}(t)$ Watts, we can now formulate the final power balance in the room using (A6). The input power is balanced by the increase in energy/second in volume V and the losses at the walls,

$$P_{in}(t) = V\frac{dW}{dt} + \frac{c}{4}A'W \text{ [W]} \tag{A7}$$

The solution to this equation is

$$W(t) = \frac{1}{V}\int_0^t P_{in}(t-t')e^{-t'/\tau}dt' \tag{A8}$$

(A8)

where $$\tau = \frac{4V}{cA'} \tag{A9}$$

is the reverberation time.

Assuming a rectangular pulse of unit height and width Δ, we find

$$W(t) = \frac{\tau}{V} e^{-t/\tau} (e^{\Delta/\tau} - 1) \qquad \text{(A10)}$$

In our case $\Delta << \tau$, so

$$\begin{aligned} W(t) &= \frac{\Delta}{V} e^{-t/\tau} \qquad t \geq t_0 \\ &= 0 \qquad\qquad t < t_0 \end{aligned} \qquad \text{(A11)}$$

since causality requires that there is a propagation delay, where $t_0 = d/c$ (Figure 1).

In order to find P_{rec}, the total power received at the antenna, we need to integrate over the tail of the impulse response and multiply the intensity with the absorption cross section of the antenna. The latter equals $\lambda^2/4\pi$ since the gain of any lossless antenna in a uniform, random environment, is 1. This leads to the final result for the path gain

$$\begin{aligned} \frac{P_{rec}}{P_{in}} = \frac{P_{rec}}{\Delta} &= \int_{t_0}^{\infty} \frac{\lambda^2}{4\pi} I(t)\, dt \\ &= \frac{\lambda^2 c}{(4\pi)^2 V} \int_{t_0}^{\infty} e^{-t/\tau} dt \\ &= \frac{\lambda^2 c \tau}{(4\pi)^2 V} e^{-t_0/\tau} \\ &= \frac{\lambda^2}{4\pi^2 A'} e^{-t_0/\tau} \end{aligned} \qquad \text{(A12)}$$

Realizing that the antenna only receives half of the incident intensity, which is assumed equally divided between two orthogonal polarizations, we multiply with a polarization factor $\eta_{pol} = 0.5$.

$$\frac{P_{rec}}{P_{in}} = \frac{\lambda^2}{4\pi^2 A'} e^{-t_0/\tau} \eta_{pol} = \frac{\lambda^2}{8\pi^2 A'} e^{-t_0/\tau} \qquad \text{(A13)}$$

The result is surprisingly simple, telling that the mean received diffuse power may be determined everywhere by knowing the reverberation time and the volume, which determine the effective absorption area A'.

It is interesting also to determine P_m (Fig. 1) where the slope cuts the power axis. Translating the zero energy density value $W(0)$ to received power, we find

$$P_m = \frac{\lambda^2}{(4\pi)^2} \frac{c\Delta}{V} \eta_{pol} \qquad \text{(A14)}$$

where the approximation in (A11) has been used. Note the independence of absorption.

ACKNOWLEDGMENT

The authors are grateful to Dr. Wolfgang Fischer and M. Schirrmacher from Airbus Germany GmbH for their permission to use the measurement data derived from the project KABTEC S11 UWB/CAMASUTRA WP08 for further study. Also, we would like to thank I. Schmidt and J. Schüür from Department of Electromagnetic Compatibility, Technische Universität Braunschweig, Germany, for their assistance in preparing and carrying out the measurements presented in this paper. Prof. R. G. Vaughan is thanked for a careful reading of the manuscript.

REFERENCES

[1] H. Hashemi, "The indoor radio propagation channel", *Proc. IEEE,* vol. 81, no. 7, 1993, pp. 943-968.

[2] A. A. M. Saleh, R. A. Valenzuela, "A statistical model for indoor multipath propagation", *IEEE Journal on Selected Areas in Communications*, vol. SAC-5, no. 2, Feb. 1987, pp. 128-137.

[3] H. El-Sallabi, D. S. Baum, P. Zetterberg, P. Kyösti, T. Rautiainen, C. Schneider, "Wideband spatial channel model for MIMO systems at 5 GHz in indoor and outdoor environments", *IEEE VTC 2006-Spring*, 2006, pp 2916 -2921.

[4] S. S. Ghassemzadeh, R. Jana, C. W. Rice, W. Turin, V. Tarokh, "Measurement and modeling of an ultra-wide bandwidth indoor channel," *IEEE Trans. Commun.*, vol. 52, no. 10, Oct. 2004, pp. 1786-1796.

[5] S. S. Ghassemzadeh, L. J. Greenstein, T. Sveinsson, A. Kavčić, V. Tarokh, "UWB delay profile models for residential and commercial indoor environments", *IEEE Trans Veh. Technol.,* vol. 54, no. 4, July 2005, pp. 1235-1244.

[6] A. F. Molisch, J. R. Foerster, M. Pendergrass, "Channel models for ultrawideband personal area networks," *IEEE Wireless Communications*, Dec. 2003, pp. 14-21.

[7] O. Franek, J. B. Andersen, G. F. Pedersen, "Diffuse scattering model of indoor wideband propagation", *IEEE Trans. Antennas Propagation, vol* 59, no 8, August 2011,pp 3006-3012.

[8] R. S. Thomä, M. Landmann, G. Sommerkorn, A. Richter, "Multidimensional high-resolution channel sounding in mobile radio", *Instrumentation and Measurement Technology Conference, IMTC 04.* vol.1, 2004, pp. 257-262.

[9] F. S. de Adana, O. G. Blanco, I. G. Diego, J. P. Arriaga, M. F. Catedra, "Propagation model based on ray tracing for the design of personal communication systems in indoor environments," *IEEE Trans. Veh. Technol.,* vol. 49, no. 6, Nov. 2000, pp. 2105-2112.

[10] Y. Zhao, Y. Hao, C. Parini, "FDTD characterization of UWB indoor radio channel including frequency dependent antenna directivities", *IEEE Antennas and Wireless Propagation Letters,* vol. 6, 2007, pp. 191-194.

[11] J. B. Andersen, J. Ø. Nielsen, G. F. Pedersen, G. Bauch, M. Herdin, "The large office environment - measurement and modeling of the wideband radio channel", *IEEE 17th International Symposium on Personal, Indoor and Mobile Radio Communications,* 11-14 Sept. 2006, pp. 1-5.

[12] J. B. Andersen, J. Ø. Nielsen, G. F. Pedersen, G. Bauch, M. Herdin, "Room electromagnetics", *IEEE Antennas and Propagation Magazine*, vol. 49, no. 2, April 2007, pp. 27-33.

[13] H. Kuttruff, *Room acoustics,* Spon Press, 2000.

[14] D. A. Hill, M. T. Ma, A. R. Ondrejka, B. F. Riddle, M. L. Crawford, T. T. Johnk, "Aperture excitation of electrically large, lossy cavities", *IEEE Transactions Electromagnetic Compatibility*, vol. 36, no. 3, August 1994, pp. 169-178.

[15] M. Jacob, K. L. Chee, I. Schmidt, J. Schüür, W. Fischer, M. Schirrmacher, T. Kürner, "Influence of passengers on the UWB propagation channel within a large wide-bodied aircraft", *3rd European Conference on Antennas and Propagation*, March 2009, Berlin, pp. 882-886.

[16] K. L. Chee, M. Jacob, T. Kürner, "A systematic model for UWB channel modeling in aircraft cabins", IEEE *Veh. Technol. Conf., VTC 2009-Fall,* 2009, pp. 1-5.
[17] S. Chiu, D. G. Michelson, "Effect of human presence on UWB radiowave propagation within the passenger cabin of a midsize airliner", *IEEE Trans on Antennas and Propagation*, vol. 58, no. 3, March 2010, pp. 917–926.
[18] S. Chiu, J. Chuang, and D. G. Michelson, "Characterization of UWB channel impulse responses within the passenger cabin of a Boeing 737-200 aircraft", *IEEE Trans Antennas Propag.*, vol 58, no. 3, Mar. 2010, pp. 935–945.
[19] C. W. Kim, X. Sun, L. C. Chiam, B. Kannan, F. P. S. Chin, H.K. Garg, "Characterization of ultra-wideband channels for outdoor office environment", Proc. *IEEE WCNC*, 13-17 Mar. 2005, pp. 950-955.
[20] K. W. Hurst, S. W. Ellingson, "Path loss from a transmitter inside an aircraft cabin to an exterior fuselage-mounted antenna", *IEEE Transactions Electromagnetic Compatibility*, vol. 50, no. 3, Aug. 2008, pp. 504-512.
[21] A. Hirata, Y. Nagaya, F. Osamu, T. Nagaoka, S. Watanabe, "Correlation between absorption cross section and body surface area of human for far-field exposure at GHz bands", *IEEE Symposium on Electromagnetic Compatibility*, 2007, pp.1-4.
[22] G. Vermeeren, W. Joseph, C. Olivier, L. Martens, "Statistical multipath exposure of a human in a realistic electromagnetic environment", *Health Physics*, vol. 94, no. 4, Apr. 2008, pp 345-354.
[23] A. Ishimaru, *Electromagnetic wave propagation, radiation, and scattering,* Prentice Hall, 1991.

Jørgen Bach Andersen (M'68–SM'78–F'92–LF'02) received the M.Sc. and Dr. Techn. degrees from the Technical University of Denmark (DTU), Lyngby, Denmark, in 1961 and 1971, respectively. In 2003 he was awarded an honorary degree from Lund University, Sweden. From 1961 to 1973, he was with the Electromagnetics Institute, DTU and since 1973 he has been with Aalborg University, Aalborg, Denmark, where he is now a Professor Emeritus and a consultant.
He has been a Visiting Professor in Tucson, Arizona, Christchurch, New Zealand, Vienna, Austria, and Lund, Sweden. From 1993-2003, he was Head of the Center for Personkommunikation (CPK), dealing with modern wireless communications. He has published widely on antennas, radio wave propagation, and communications, and has also worked on biological effects of electromagnetic systems. He was on the management committee for COST 231 and 259, a collaborative European program on mobile communications.
Professor Andersen is a Life Fellow of IEEE and a former Vice President of the International Union of Radio Science (URSI) from which he was awarded the John Howard Dellinger Gold Medal in 2005.

Gert Frølund Pedersen received the B.Sc. E.E. degree in electrical engineering (Hons.) from the College of Technology, Dublin, Ireland, in 1991,and the M.Sc. E.E. and Ph.D. degrees in electrical engineering from Aalborg University, Aalborg, Denmark, in 1993 and 2003, respectively. Currently, he is a Full Professor and heads the Antennas, Propagation and Radio Networking (APNet) Group at Aalborg University. His research has focused on radio communication for mobile terminals, including small antennas, antenna systems, propagation, and biological effects. He has been published in many publications including more than 15 patents. He was also a Consultant with small antennas and developed more than 50 dedicated designs for small mobile terminals starting with the first internal antenna for mobile phones in 1993 with very low specific absorption rate. The first internal triple-band antenna in 1998 with low SAR and high efficiency and various antenna diversity systems were rated as the most efficient on the market. He has recently been involved in establishing the method to measure over-the-air (OTA) communication performance for mobile terminals adopted by 3G Partnership Project (3GPP) for measurements that include the antenna. Further, he is involved in small terminals for fourth generation, including several antennas (multiple-input, multiple-output (MIMO) systems) and ultra wideband antennas to enhance data communication. Prof. Pedersen is the Chairman of COST 2100 SWG 2.2, which is working on the upcoming OTA standard for multiantenna terminal testing for 3GPP and CTIA.

Kin Lien Chee (M'10) was born in Pahang, Malaysia. He received the B.Eng. (Hons.) in electrical and electronics engineering in 2003, from the Nanyang Technological University, Singapore and M.Sc. in electronics engineering from the University of Applied Sciences Bremen, Germany, in 2008.
From 2003 to 2006, he worked at Smith Detection Asia Pacific in Singapore and Australia, dealing with baggage inspection system using X-ray technology in aviation, ports and borders. From 2008 to present, he is a researcher at the Institut für Nachrichtentechnik, Technische Universitaet Braunschweig, Germany, working on radio wave propagation for broadband wireless access system in rural residential areas. He has been a member of the COST 2100 and IC1004 initiatives.

Martin Jacob (S'08) was born in Bielefeld, Germany, in 1982. He received the Dipl.-Ing. degree in Electrical Engineering from the Technische Universität Braunschweig in 2007. Currently, he is pursuing his Ph.D. as a research assistant with the Institut für Nachrichtentechnik at Technische Universität Braunschweig. He is the author of more than 30 technical journal and conference papers in the field of system and channel modeling for UWB, GPS, mm-wave and THz systems. His current research interest lies in the field of wireless communication systems at frequencies of 60 GHz and above. His work mainly focuses on channel and propagation modeling as well as propagation measurements. He is a contributor to the IEEE 802.11ad 60 GHz WLAN channel model and has been a member of the COST 2100 and IC1004 initiatives. Mr. Jacob received the 2011 URSI Commission B Young Scientist Award.

Thomas Kürner (S'91-M'94-SM'01) received the Dipl.-Ing. degree in Electrical Engineering from Universitaet Karlsruhe (Germany) in 1990 and the Dr.-Ing. degree in 1993 from the same university. From 1990 to 1994 he was with the Institut fuer Hoechstfrequenztechnik und Elektronik (IHE) at the Universitaet Karlsruhe working on wave propagation modeling, radio channel characterization and radio network planning. From 1994 to 2003 he was with the radio network planning department at the headquarters of the GSM 1800 and UMTS operator E-Plus Mobilfunk GmbH & Co KG, Duesseldorf, where he was team manager radio network planning support being responsible for radio network planning tools, algorithms, processes and parameters. Since 2003 he has been a Professor for Mobile Radio Systems at the Institut fuer Nachrichtentechnik (IfN) at Technische Universitaet Braunschweig. His working areas are propagation, traffic and mobility models for automatic planning of mobile radio networks, planning of hybrid networks, car-to-car communications as well as indoor channel characterization for high-speed short-range systems including future terahertz communication systems. He has been engaged in several international bodies such as ITU-R SG 3, UMTS Forum Spectrum Aspects Group and COST 231/ 273/ 259/ 2100. He has been participant in the European projects IST-MOMENTUM and ICT-SOCRATES. Currently, he is chairing IEEE802.15 IG THz. He has served as Vice-Chair Propagation at the European Conference on Antennas and Propagation (EuCAP) in 2007 and 2009 and has been Associate Editor of IEEE Transactions on Vehicular Technology since 2008. He is a member of VDE/ITG, VDI, Senior Member of the IEEE and an elected member of the International Scientific Radio Union (URSI/USNC) Commission F (Radio Wave Propagation and Remote Sensing).